*Sensors & Transducers, Vol. 266, Issue 3, August 2024, pp. 16-24*

www.sensorsportal.com

**Sensors & Transducers**

Published by IFSA Publishing, S. L., 2024
http://www.sensorsportal.com

# Thin-film Interference Demultiplexer for VIS-WDM

*** Ulrich H. P. FISCHER and Mladen JONČIĆ**
Harz University of Applied Sciences, 38855 Wernigerode, Germany
Tel.: +49 152 5363 5589
* E-mail: ufischer@hs-harz.de

*Received: 24 April 2024 / Revised: 3 July 2024 / Accepted: 5 August 20204 / Published: 12 April 2024*

**Abstract:** In short-range communication 1 mm PMMA Step Index Polymeric Optical Fibers established itself as a reasonable. alternative to the traditional data communication media such as glass fibers, copper cables and wireless systems. Due to multiple advantages such as a large core diameter, tolerance to fiber facet damages and low installation costs, the SI-POF is typically used for network systems in homes, vehicles and industrial automation. For wavelength division multiplex an optical demultiplexer is a key component. The paper concentrates on the demultiplexing techniques employing thin-film interference filters used in Polymeric Fiber Transmission Systems. An interference filter-based Step Index Polymeric Optical Fibers demultiplexer was realized using a precisely adjustable. opto-mechanical setup, which allowed maximization of the optical throughput in the individual channels. Intermediate setups with two and three channels were first established. In addition, a serial and a two-stage configuration of a target setup with four channels were realized. It was shown that the latter configuration outperformed the former one in terms of Insertion Loss (IL) and IL uniformity. Furthermore, the demultiplexer with two-stage configuration provided low insertion loss (< 5.7 dB) and high channel isolation (> 30 dB). It outperformed other interference filter- based SI-POF demultiplexers reported so far, and was well suited for implementation in high- speed POF WDM transmission experiments. To demonstrate experimentally the feasibility and potential of a high-speed POF WDM concept, a four-channel data transmission setup was realized.

**Keywords:** Polymeric fiber transmission systems, WDM transmission, Interference demultiplexer, POF-multiplexer.

## 1. Introduction

Polymeric Optical Fibers (POF) is very attractive for the use in short-range telecommunication networks. Among different types of POF, the standard 1-mm diameter Step Index-POF is the best known and by far the most widely used type of POF. SI-POF offers many advantages in comparison to alternative data communication media such as glass fibers, copper cTab.s, and wireless systems. It is pliTab., durTab., and inexpensive, offers small weight and short bend radius, allows easy installation and quick troubleshooting, and also provides the immunity to electromagnetic interference. Due to its numerous advantages SI-POF is already applied in various application sectors (in-house networks, automotive and aerospace industry, industrial control, etc.) [1].

Present communication systems over POF use a single channel for data transmission. Commercial systems with SI-POF can deliver a bandwidth of 250 Mbit/s over 50-100 m. Multi-Gbit/s transmission over SI-POF was demonstrated in the laboratory conditions [2]. However, the standard SI-POF has the lowest capacity among all POFs due to the strong inter-modal dispersion and high attenuation [3].

To increase the capacity of a single POF, multiple optical carriers can be used for parallel transmission of communication channels over the same fiber. The technique is known as Wavelength Division Multiplex (WDM). In glass fiber communications WDM has already been firmly established for two decades, and represents the key technology in modern long- and medium-haul optical communication systems [4].

A growing interest to develop WDM components and systems for POF is present in recent years [5]. WDM technology for POF is already under investigation by several working groups [6-8]. The development of the key WDM components (e.g.

DEMUX: Demultiplexer, MUX: Multiplexer) (Fig. 1) is essential to the success of WDM over POF. It is also important to define a unique set of WDM transmission channels for the realization of standardized commercial WDM devices and systems for POF. A principle of an WDM structure is depicted in Fig. 1.

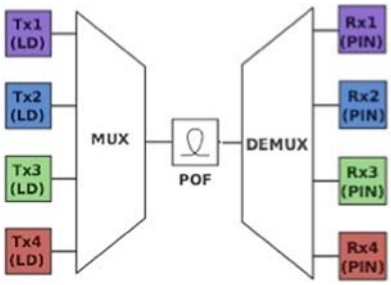


**Fig. 1.** Basic structure of an optical four-channel WDM transmission system over POF with its components.

In [9, 10] the extension of *Coarse* WDM grid (according to ITU-T G.694.2 Rec. [11] into the visible spectrum was proposed as a spectral grid for CWDM applications over SI-POF in [9].

The working group at the Harz University is working about the key-components for high-speed communication over POF, especially optical MUX/DEMUX element, are researched and developed in the project HOPE (*High Speed Optical Transmission Systems using Polymeric Fibers*) of the German Federal Ministry of Research [12]. One goal of this project is the realization of a low-cost grating based DEMUX in injection molding technology [13, 14]. Another goal of the project is the investigation and realization of a 10 Gbit/s four-channel CWDM transmission system over 50 m SI-POF link using interference filters. Course WDM in the visible region of our experiment means channel spacings of 20 nm – 100 nm.

## 2. Transmission Properties of 1 mm PMMA SI-POF

The 1 mm PMMA SI-POF is the best known and by far the most widely employed type of POF. It is made of 980 µm diameter PMMA core surrounded by a thin cladding (10 µm) made of fluorinated polymer. The typical spectral attenuation of SI-POF is shown in Fig. 2. The fiber supports operation in the visible spectrum from 400 nm to 700 nm. The lower wavelength bound is determined by the degradation of the PMMA compound with prolonged exposure to the ultraviolet (UV) wavelengths [15]. The attenuation value of around 400-450 dB/km, that still allows operation over shorter link lengths (< 20 m), sets the upper wavelength bound.

Two intrinsic loss mechanisms contribute to the raise of attenuation at shorter and particularly UV wavelengths. The electronic transitions due to the absorption of light in the polymer compound cause absorption peaks in the UV region. However, their absorption tails extend through the visible spectrum affecting the POF attenuation [16]. The dependence of the attenuation coefficient of electronic transitions $\alpha_e$ [dB/km] on the wavelength for PMMA is given by [17]:

$$\alpha_e = 1.58 \cdot 10^{-12} \, exp\left(\frac{1.15 \cdot 10^4}{\lambda}\right) \quad (1)$$

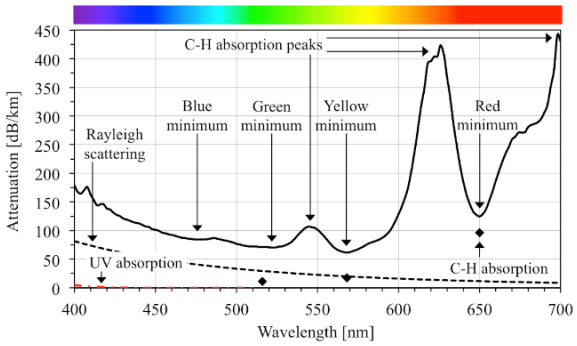


**Fig. 2.** Typical spectral attenuation of 1 mm PMMA SI-POF [18] with contributions of intrinsic loss mechanisms and with attenuation minima and maxima.

The second loss mechanism is the Rayleigh scattering. It is caused by the structural irregularities in the polymer compound that are much smaller than the wavelength of light (order of one tenth of wavelength or less). The effect of scattering becomes more pronounced as the wavelength decreases since the scattering attenuation coefficient $\alpha_s$ [dB/km] is inversely proportional to the fourth power of the wavelength [19]:

$$\alpha_s = 13 \cdot \left(\frac{633}{\lambda}\right)^4 \quad (2)$$

In the infrared region the attenuation significantly increases due to the intrinsic absorption losses caused by vibrations of the molecular C-H bonds (total of eight per MMA monomer). The higher overtones of the C-H bond vibrations also extend in the visible spectrum. The 7th overtone at 549 nm, and particularly the 6th and the 5th overtone at 627 nm and 736 nm respectively, cause pronounced absorption peaks and wide absorption bands, predominantly determining the level of attenuation in the red spectral range [20, 21].

The contributions of the intrinsic loss mechanisms to the overall attenuation of SI-POF are also shown in Fig. 2. The attenuation contributions due to the vibrations of C-H bonds at 516 nm, 568 nm and 650 nm are taken from [19]. The sum of individual intrinsic loss mechanisms corresponds to the theoretical loss limit and equals approx. 40 dB/km, 37 dB/km and 107 dB/km at the respective wavelengths. In practice is this limit never achieved due to the extrinsic loss processes (absorption due to

impurities in the fiber core, scattering loss due to waveguide structural imperfections, etc.) [16].

The wavelength regions where the fiber exhibits low attenuation are called attenuation windows. The SI-POF has four attenuation windows. Those are blue, green, yellow and red windows, with the absolute attenuation minimum of approx. 62 dB/km at around 568 nm (yellow window). The parameters of the attenuation windows are listed in Table 1.

**Table 1.** Attenuation windows of SI-POF (based on the attenuation curve from Fig. 2.

| Attenuation window | blue | green | yellow | red |
|---|---|---|---|---|
| Attenuation minimum [dB/km] | 85 | 70 | 62 | 125 |
| Wavelength of the attenuation minimum [nm] | 476 | 522 | 568 | 650 |
| Approximate 3 dB width of the window [nm] | 19 | 24 | 8 | 4 |

The mean refractive index of SI-POF core material in the visible spectrum is $n_{core}$ = 1.492, whereas the refractive index of cladding is $n_{clad}$ = 1.412. Due to the big difference in refractive indices of core and cladding, the numerical aperture (NA)

$$NA = \sqrt{n_{core}^2 - n_{clad}^2} \quad (3)$$

has the value of 0.482 (usually rounded to 0.5). The corresponding maximum acceptance angle of the fiber is 30º. The large core radius $a_{core}$ = 490 µm combined with the high NA results in the normalized frequency $V$:

$$V = 2\pi \frac{a_{core}}{\lambda} \cdot NA \quad (4)$$

of 2698 at 550 nm, which is far above the limit $V$ = 2.405 below which a fiber is single-moded. The number of modes $N_{mod}$ propagating through SI-POF can be approximated as

$$N_{mod} \approx V^2/2, \quad (5)$$

corresponding to 3.64 million modes at 550 nm. Due to the significant path difference between lower and higher order modes, propagating respectively at smaller and larger angles relative to the optical axis, the strong intermodal dispersion is inherent to SI-POF. In the time domain it is manifested as pulse broadening, thus introducing the inter-symbol interference (ISI). In the frequency domain the intermodal dispersion results in a low pass frequency response, constraining the bandwidth-length product of SI-POF to around 50 MHz × 100 m [22].

## 3. Demultiplexing for 1 mm PMMA SI-POF

The WDM is one possibility to increase the data carrying capacity of SI-POF. The key component for WDM is a wavelength demultiplexer. Different approaches for realization of the demultiplexer for SI-POF have been investigated, including demultiplexing based on a dispersion prism, thin-film interference filters, and a diffraction grating (plane or concave).

The prism-based two-channel demultiplexer operating with LEDs at 530 nm and 650 nm was reported in [23]. The insertion loss (IL) and the crosstalk were around 17-20 dB and -20 dB respectively. Another solution employing the dispersion prism was shown in [24]. The three-channel demultiplexer operated with LEDs at 470 nm, 520 nm and 650 nm. It provided the IL of 12-20 dB, whereas the crosstalk took values between -4.6 dB and -34.8 dB. High IL and considerable crosstalk were caused by unoptimized optical components, broad LED spectra and high alignment sensitivity of both setups.

The two other demultiplexing techniques have been recognized as the most promising for SI-POF and have been the most investigated so far. This work focuses on the demultiplexers employing interference filters.

### 3.1. Demultiplexing Employing Thin-film Interference Filters

The technology based on thin-film interference filters is mature and one of the most commonly applied technologies for realization of WDM demultiplexers in single-mode glass fiber communication. The demultiplexers for *Coarse* WDM applications cascade the interference filters to provide up to 16 flat-top channels between 1271 nm and 1611 nm, with 20 nm minimum channel spacing [25]. The typical parameters of commercial 4-, 8-, and 16-channel demultiplexers with IL less than 1.6 dB, 2.7 dB and 3.7 dB respectively, can be found in [26]. The thin-film filter-based demultiplexers for *Dense* WDM applications are commercially available. with up to 40 channels in 1550 nm region and less than 8 dB IL. Instead of simply cascading the filters, those devices usually employ a modular configuration described in [27]. The same reference provides a typical transfer function of the 40-channel demultiplexer with 3-6 dB IL and 100 GHz (0.8 nm) channel spacing.

In the visible spectrum, and thus within the application range of SI-POF, a vast variety of thin-film interference filters is available from various manufacturers. Even though not particularly intended for POF applications, the visible interference filters represent an attractive solution for POF demultiplexers, where wavelength selectivity, low IL and high isolation are required.

An interference filter, typically designed for 0º angle of incidence (AOI), utilizes the principle of constructive and destructive interference to selectively transmit certain wavelengths and reject (diminish in intensity and reflect) the others [28]. Its basic structure comprises multiple thin dielectric layers with alternating high and low refractive indices, which are successively deposited on a single glass substrate. The desired spectral response is obtained by a careful selection of the number of dielectric layers, their thickness and refractive indices. The filter is typically characterized with high passband transmittance (> 90 %), steep transition slopes (> 3 dB/nm) and deep blocking (> 30 dB) in rejection bands (see Fig. 3).

**Table 2.** Basic parameters of hard-coated bandpass interference filters from Edmund Optics utilized in different demultiplexer setups (datasheet information).

| Center wavelength [nm] | 405 | 450 | 525 | 640 | 650 | 660 |
|---|---|---|---|---|---|---|
| 3 dB passband bandwidth [nm] | 10 | 10 | 50 | 10 | 50 | 10 |

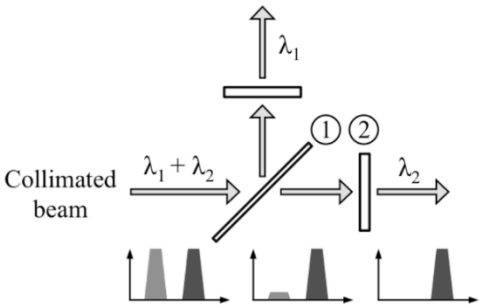


**Fig. 3.** Principle of separation of two collimated wavelength channels employing thin-film interference filters: 1 is the dichroic mirror (45º AOI); 2 is the interference filter (0º AOI).

A dichroic mirror is a special type of interference filter intended for the spatial separation or combination of light at different wavelengths. It is designed to operate at 45º AOI, such that a certain spectral range is transmitted, whereas the rejected wavelength range is reflected at 90º angle with respect to the incident optical axis. A commercial visible spectrum dichroic mirror has a transition slope between the transmission and reflection band of typically 30-40 nm (see Figs. 4, 5 and Table 3).

This is significantly less steep compared to the standard interference filters designed for the normal incidence. Unlike an interference filter, e.g. a long pass mirror must be not only highly transmissive above the cutoff wavelength, but also highly reflective below it. Therefore, producing steeper slopes would require increased complexity of the coating, and accordingly, a significant rise in production costs.

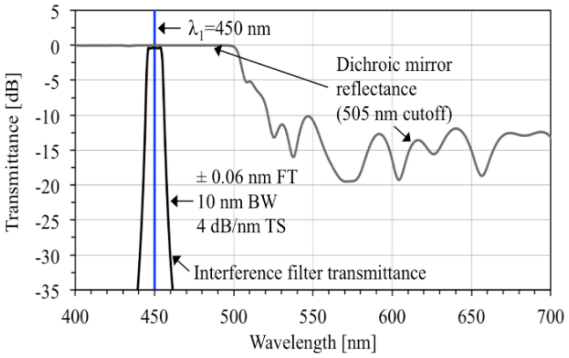


**Fig. 4.** Selection of the dichroic mirror and interference filters for demultiplexing two wavelength channels centered around $\lambda_1$ = 450 nm.

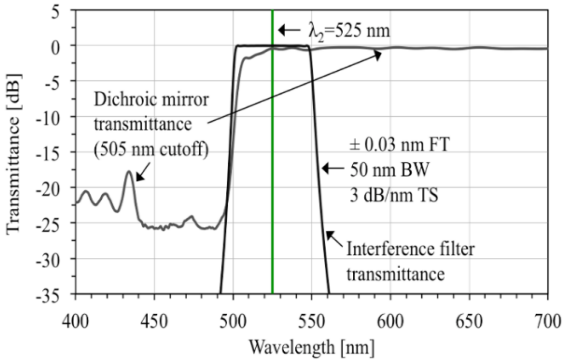


**Fig. 5.** Selection of the dichroic mirror and interference filters for demultiplexing two wavelength channels centered around $\lambda_2$ = 525 nm.

**Table 3.** Basic parameters of hard-coated dichroic mirrors utilized in different demultiplexer setups (datasheet information).

| **Type** | | **Long-pass** | | **Short-pass** |
|---|---|---|---|---|
| Cutoff wavelength [nm] | 425 | 505 | 567 | 650 |
| Transmission band [nm] (> 85 %) | 440-700 | 520-700 | 584-700 | 400-630 |
| Reflection band [nm] (> 90 %) | 380-410 | 380-490 | 380-550 | 675-850 |
| Manufacturer | Thorlabs | Edmund Optics | | |

The interference filters show significant angular dependence of their transmission characteristic [29]. To be applicable for SI-POF, the highly divergent beam from the fiber must be transformed into a bundle of parallel rays prior to the incidence. The principle of separation of two collimated wavelength channels using a dichroic mirror is shown in Fig. 1. To increase the channel isolation, an additional bandpass filtering in each of the output channels should be implemented prior to the focusing of light. As an example, a selection of the dichroic mirror and interference filters for demultiplexing two wavelength channels centered

around $\lambda_1$ = 450 nm and $\lambda_2$ = 525 nm is shown in Figs. 4 and 5.

There were several attempts to realize an SI-POF demultiplexer with interference filters. The three-channel demultiplexer for the blue, green and red wavelength regions, shown in [30] offered the IL of 7-10 dB. Another three-channel solution with wide channel passbands in the violet, green and red spectral regions was reported in [31]. The device provided the IL of 6-7 dB and high channel isolation. By far the best three-channel demultiplexer was reported in [32]. It had wide (> 50 nm) channel passbands in the violet/blue, green and red spectral regions, the IL as low as 2.5 dB (at 570 nm), and high isolation between the channels (> 30 dB). At 450 nm, 520 nm and around 650 nm (lasing wavelengths used for SI-POF communication and in this thesis) the IL was 5 dB, 3 dB and 3 dB respectively. The demultiplexer offered small dimensions by employing a plastic housing with slits for lenses and dichroic mirrors. Furthermore, it allowed easy connection of the input and the output fibers to the housing.

In the patent [33] the same authors as in [34] proposed the design of a four-channel demultiplexer by cascading the dichroic mirrors. To the best of author's knowledge, no information about practical realization of the setup has ever been published. The only four-channel demultiplexer realized so far was shown in [35]. It was based on a two-stage configuration and operated with LEDs at 470 nm, 520 nm, 590 nm and 650 nm. The IL of the setup was estimated to be 4-5 dB, but no transfer function was provided by the author. Since no additional filtering was implemented in the output ports, the demultiplexer experienced very high crosstalk. Therefore, it could not be used as a stand-alone component, but rather in combination with an electronic crosstalk compensation.

When properly designed, an interference filter-based demultiplexer is capable. of providing low IL and high isolation. That makes it suitable. for realizing and investigating POF WDM communication systems. In the thesis this demultiplexing approach for SI-POF is further investigated. The goal is to increase the channel count compared to [30, 36] and [34], and realize a four-channel demultiplexer with improved performances compared to [35].

## 4. Key WDM Components

The realization of high-speed POF WDM systems requires high-speed high-power visible LDs. Recent development progress brought to the market different violet, blue, green, and red LDs. A wavelength MUX and DEMUX for the visible spectrum are indispensable photonic components in a CWDystem under development. These have been recently realized at the Harz University. In this section, we give an overview of acquired LDs. In addition, developed MUX and DEMUX are presented in [37].

### 4.1. Laser Diodes

The basic parameters of LDs used in our WDM system are listed in Table 4 and shown in Figs. 6 and 7 The commercially available LDs at 405 nm, 450 nm, and 639 nm operate in WDM channels 1, 2, and 4 respectively. The 514 nm research and development sample is assigned to channel 3.

**Table 4.** Parameters of Laser Diodes used in WDM system.

| MUX input port / WDM channel | 1 | 2 | 3 | 4 |
|---|---|---|---|---|
| Launching coupling loss + 400-µm fiber attenuation [dB] | 4.89 | 4.93 | 4.63 | 4.56 |
| Connector loss [dB] | 0.1 | 0.58 | 0.22 | 0.3 |
| Total loss [dB] | 4.99 | 5.51 | 4.85 | 4.86 |

**Fig. 6.** LD soldered to a formable coax cable.

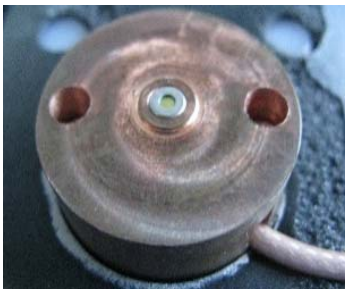

**Fig. 7.** LD mounted in a copper retainer ring.

### 4.2. Multiplexer

POF couplers can be used to efficiently combine signals with different wavelengths onto a single fiber. The multiplexing function of a 4:1 coupler is shown in Figs. 8, 9 and 10.

To multiplex the output beams of the LDs, a simple 4:1 POF coupler has been realized with commercially available components. Four 60 cm long 400-µm diameter PMMA SI-POFs with installed 400-µm diameter FC connectors were used as the input ports. The LDs were butt-coupled to these fibers by means of a coupling unit. On the link side, the 400-µm fibers were glued together in a standard 1-mm diameter FC connector to form the MUX output port at the connector end face.

To connect the MUX output port to the 1-mm diameter SI-POF link, a simple FC connector coupling was used with index matching gel between the connector end faces.

To optimize the MUX design, a 970-µm diameter FC connector should be used at the output port. The mechanical and optical set-up is depicted in Figs. 9 and 10.

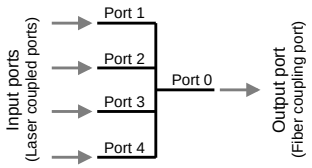


**Fig. 8.** Multiplexing function of 4:1 coupler.

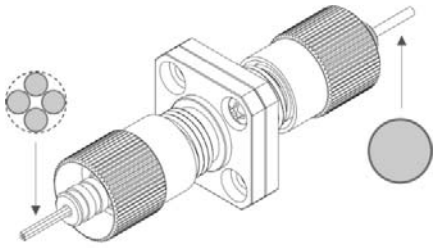

**Fig. 9.** Four-legged multiplexing POF bundle set-up with FC connector.

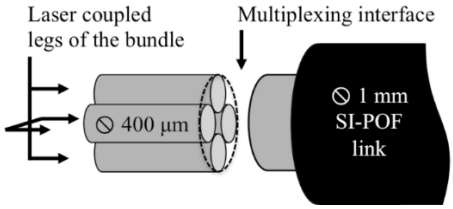


**Fig. 10.** Cross section of 4 400 µm fibers and 1 mm fiber.

The insertion loss (IL) of the MUX, consisting of launching coupling loss, 400-µm fiber attenuation, and connector loss, is given in Table 5.

**Table 5.** Insertion loss of the MUX.

| WDM channel | 1 | 2 | 3 | 4 |
|---|---|---|---|---|
| Emission wavelength [nm] | 405 | 450 | 514 | 639 |
| Opt. output power [dBm] | 16 | 19 | 17 | 10 |
| Threshold current [mA] | 35 | 30 | 60 | 30 |
| Operating current [mA] | 70 | 100 | 160 | 40 |

## 4.3. Demultiplexer

Different proposals for the realization of the DEMUX for SI-POF have been reported in the past. Except one (four-channel), all of the realized DEMUXs were two-channel or three-channel solutions. A good overview of these proposals can be found in [3, 10, 8, 13]. Three main approaches for DEMUX realization were prism-based, filter-based, and grating-based DEMUX.

A four-channel filter-based DEMUX has been realized in the bulk optics technology at the Harz University. The principle of operation of the DEMUX is shown in Fig. 11. A multi-wavelength light beam exiting the sending fiber end face is first collimated by means of an aspheric lens. Dichroic mirrors used in the DEMUX are designed for the use at a 45° angle of incidence. The first dichroic mirror (colored orange) reflects violet and blue while transmitting green and red spectral portion of the incidence light beam. The second dichroic mirror (colored blue) reflects violet while transmitting blue, and the third dichroic mirror (colored red) reflects green while transmitting red spectral portion of the incidence light beam. Interference filter is placed in each channel to reduce the crosstalk and to narrow the channel passband. Filtered light beam is then focused on the receiving fiber end face by means of an aspheric lens, and fed to the receiver.

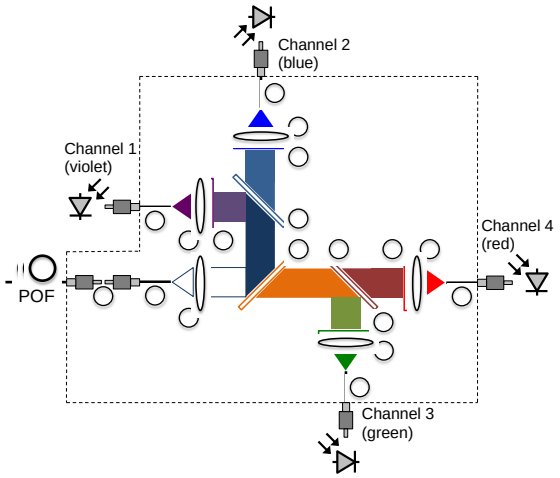


**Fig. 11.** Principle of operation of a four-channel DEMUX: 1 is the FC connector coupling; 2 is the 1 m SI-POF; 3 is the aspheric lens; 4 is the dichroic mirror; 5 is the interference filter.

The basic DEMUX parameters are summarized in Table 6.

The realized DEMUX supports the spectral grid proposed in [6, 7, 9] by showing that it is possible to realize channels with narrow passbands (< 10 nm).

To the best of author's knowledge, high number of channels, low IL, and high isolation make this DEMUX the best DEMUX solution for SI-POF reported so far.

The fiber coupled power, the power at the output of the 25 m SI-POF link and the received power at DEMUX output ports are shown in Table 7 and the spectrum in Fig. 12 received powers comply with the recommended maximum input optical power for

SPD-2 photoreceiver of -4 dBm. To maximize the modulation amplitude and thus the signal-to-noise ratio of the modulating signal, the longitudinal offset was introduced between the LDs and the input ports of the MUX in order to reduce the coupling efficiency and not exceed the -4 dBm limit at the receiver.

**Table 6.** Basic DEMUX parameters.

| DEMUX channel | 1 | 2 | 3 | 4 |
|---|---|---|---|---|
| Center wavelength [nm] | 404.9 | 450.1 | 528.3 | 646.4 |
| 3 dB passband bandwidth [nm] | 9.5 | 9.4 | 41.6 | 47.6 |
| IL [dB] | 5.66 | 4.55 | 3.47 | 3.19 |
| IL uniformity [dB] | 2.47 | | | |
| Adjacent / non-adjacent channel isolation [dB] | > 30 | | | |

**Table 7.** Optical power levels along CWDM link.

| WDM channel | 1 | 2 | 3 | 4 |
|---|---|---|---|---|
| Fiber coupled power [dBm] | 4.49 | 2.36 | 1.76 | 5.58 |
| Power at the output of the fiber link [dBm] | 1.51 | 0.60 | 0.35 | -0.04 |
| Power at the output of DEMUX [dBm] | -4.00 | -4.03 | -4.12 | -3.95 |

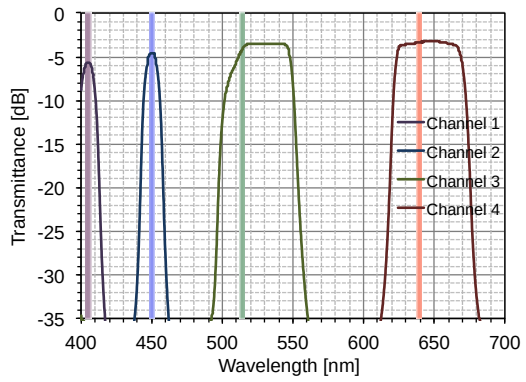


**Fig. 12.** Transfer function of developed four-channel DEMUX. Per channel includes the loss of one connector coupling, the loss of the opto-mechanical setup, and the attenuation of 2 m SI-POF. Lasing wavelengths indicated with colored vertical lines.

The IL of DEMUX at the lasing wavelengths can be calculated from Table 8 as the difference between the power at the output of the fiber link and the received power at the output of DEMUX. Table 5 gives the comparison of IL of DEMUX when it is estimated based on the transfer function and directly measured after 25 m fiber link. The absolute value of the difference does not exceed 0.55 dB, verifying the demultiplexing function when operating with LDs. It can be also noticed that the IL uniformity at the lasing wavelengths reduces from 2.3 dB for estimation based on the transfer function to 1.6 dB for LD launching.

**Table 8.** Comparison of IL of DEMUX at the lasing wavelengths.

| MUX channel | 1 | 2 | 3 | 4 |
|---|---|---|---|---|
| Lasing wavelength [nm] | 405 | 450 | 514 | 639 |
| IL estimated based on the transfer function [dB] | 5.66 | 4.56 | 4.15 | 3.36 |
| Measured IL after MUX and 25 m SI-POF [dB] | 5.51 | 4.63 | 4.47 | 3.91 |
| Δ IL [dB] | -0.15 | 0.07 | 0.32 | 0.55 |

## 5. Data Transmission Setup

The experimental setup for the investigation of four-channel CWDM systems over SI-POF is shown in Fig. 13. It is based on the offline processing approach since no commercial components are so far available. A four-channel Agilent M8190A arbitrary waveform generator (AWG) with 12-bit vertical resolution and up to 12 GSa/s sampling rate was used to convert digital data into an analog electrical signal. In the transmission experiment, the AWG generated four independent NRZ data streams with Pseudorandom Binary Sequence PRBS test pattern length of $2^7$-1 and up to 1 $V_{pp}$ modulation amplitude.

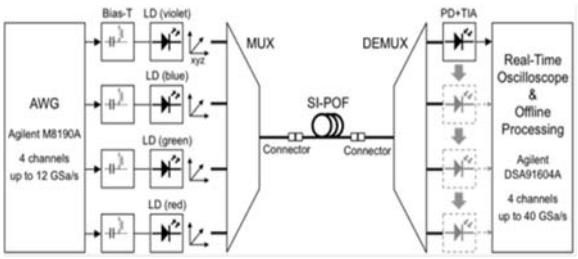


**Fig. 13.** Data transmission Setup with 25 m transmission.

The LDs were directly modulated in their linear lasing region with a modulation index of approximately 0.95. The optical link contained a MUX, 25 m standard SI-POF, and a DEMUX. A Graviton SPD-2 photoreceiver with a 1.2 GHz bandwidth was used for detection. As indicated in Fig. 13 the detection was performed channel after channel. Received signals were acquired by the Agilent DSA91604A real-time oscilloscope that has up to 80 GSa/s sampling rate and 8-bit vertical resolution. Further digital processing was carried out in the offline mode by means of the oscilloscope's

built-in software. The equalization was performed by Serial Data Equalization software. In the experiments Feed-Forward Equalization (FFE) was used and the equalized eyes were displayed on the oscilloscope's screen for further analysis. The Bit Error Rate BER was calculated based on the quality factor or Q-factor [15], shown in Figs. 14 and 15.

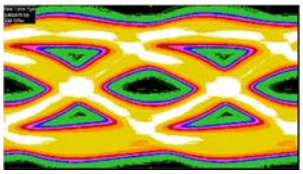

**Fig. 14.** Example 1 of measured eye diagram of Channel 3: at $R_{b3}$ = 2.6 Gbit/s with Q-factor of 3.668 resulting in BER = $1.22 \cdot 10^{-4}$.

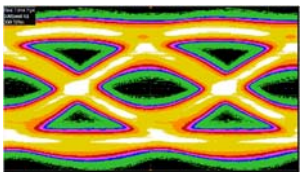

**Fig. 15.** Example 2 of measured eye diagram of Channel 4 at $R_{b4}$ = 3.5 Gbit/s with Q-factor of 4.058 resulting in BER = $2.48 \cdot 10^{-5}$.

### 5.1. Experimental Results

The reason for different values lies in the fact that different optical sources were used in these two measurements (white light source versus LDs).

A total bit rate of 10.7 Gbit/s was transmitted over four channels.

## 6. Conclusions

A growing interest and activities to develop WDM components and systems for POF are present in recent years. The development of cheap and fast optical transceivers and cheap photonic WDM components is essential to the success of WDM over POF.

The current development status of a four-channel CWDM transmission system for the investigation of multi-Gbit/s data links over SI-POF is reported in the paper. The key photonic WDM components were realized at the Harz University. For combining the optical signals coming from violet, blue, green, and red LDs onto 1-mm SI-POF a 4:1 coupler with low IL was developed. A four-channel DEMUX with low IL and high isolation was realized in the bulk optics technology. To the best of author's knowledge, high number of channels, low IL, and high isolation make this DEMUX the best DEMUX solution for SI-POF reported so far. We demonstrate a 10.7 Gbit/s four-channel WDM transmission over 25 m SI-POF link at BER of less than $10^{-3}$.

## References


[1]. U. H. P. Fischer, M. Haupt, M. Joncic, Optical transmission systems using polymeric fibers, Chapter 22, in Optoelectronics – Devices and Applcations (P. Predeep, Ed.), *Intech Open*, 2011.

[2]. R. Caspary, *et al.*, High speed WDM transmission on standard polymer optical fibers, in *Proceedings of the 17th International Conference on Transparent Optical Networks (ICTON'15)*, 2015, pp. 1-4.

[3]. O. Ziemann, J. Krauser, P. E. Zamzow, POF Handbook - Optical Short Range Transmission Systems, *Springer Verlag*, Berlin, Heidelberg, 2008.

[4]. B. Mukherjee, Optical WDM Networks, *Springer*, Berlin, Heidelberg, 2006.

[5]. O. Ziemann, S. Loquai, J. Vinogradov, R. Kruglov, The 1 gigabit over 1 mm POF story – From vision to standard, in *Proceedings of the European Conference on Optical Communication (ECOC'10)*, Vols. 1-2, 2010.

[6]. M. Joncic, M. Haupt, U. Fischer, WDM over SI-POF – a general concept, in *Proceedings of the 13. Nachwuchswissenschaftlerkonferenz mitteldeutscher Fachhochschulen*, 2012, pp. 256-261.

[7]. L. V. Bartkiv, Y. V. Bobitski, H. Poisel, Use of concave VLS grating for combining and separating of wavelength channels in POF systems, in *Proceedings of the International Conference Modern Problems of Radio Engineering, Telecommunications and Computer Science*, 2004, pp. 2-3.

[8]. R. Kruglov, J. Vinogradov, O. Ziemann, S. Loquai, C.-A. Bunge, L. Bartkiv, Potential of CWDM technology for 10 Gbit/s data transmission over SI-POF, in *Proceedings of the Intern. POF Conference*, 2012, pp. 290-295.

[9]. J. Mladen, *et al.*, Standardization proposal for spectral grid for Vis Wdm applications over Si-Pof, in *Proceedings of the 21th Int. Conference Plast. Opt. Fibers*, 2012, pp. 351-355.

[10]. M. Jon, M. Haupt, U. H. P. Fischer, M. Joncic, M. Haupt, U. H. P. Fischer, Investigation on spectral grids for VIS WDM applications over SI-POF Untersuchung von Spektralen Gittern für VIS WDM-Anwendungen über SI-POF, in *Proceedings of the ITG Fachtagung "Photonische Netze 2013" Conference*, 2014, 38855.

[11]. I.-T. G.694.2, Spectral grids for WDM applications: CWDM wavelength grid, *International Telecommunication Union*, 2002.

[12]. U. H. P. Fischer-Hirchert, *et al.*, High-speed optical in-house networks using polymeric fibers, in Broadband Communications Networks – Recent Advances and Lessons from Practice (A. Haidine, A. Aqqal, Eds.), *IntechOpen*, 2017.

[13]. M. Haupt, Wellenlängenmultiplex im sichtbaren Spektrum für optische Polymerfaser-Systeme, *Cuvillier Verlag*, Göttingen, 2010.

[14]. S. Holl, *et al.*, Injection molding of a WDM system for POF communication, in *Proceedings of the Electronic Components and Technology Conference (ECTC'13)*, 2013, pp. 2292-2297.

[15]. N. Lekishvili, L. Nadareishvili, G. Zaikov, Polymers and Polymeric Materials for Fiber and Gradient Optics, *Brill Academic Publishers*, 2002.

[16]. J. Zubia, J. Arrue, Plastic optical fibers: An introduction to their technological processes and applications, *Opt. Fiber Technol.*, Vol. 7, Issue 2, 2001, pp. 101-140.

[17]. Y. Koike, Fundamentals of Plastic Optical Fibers, *Wiley and Sons Inc*., 2014.
[18]. C.-A. Bunge, Private communication – Spectral Atenuation of Asahi Fiber Specified for MOST.
[19]. T. Kaino, Organic Molecular Solids: Properties and Applications, *CRC Press*, 1997.
[20]. C. Emslie, Review polymer optical fibers, *J. Mater. Sci.*, Vol. 23, 1988, pp. 2281-2293.
[21]. W. Groh, Overtone absorbtion in macromolecules for polymer optical fibers, *Die Makromol. Chemie*, Vol. 189, Issue 12, 1988, pp. 2861-2874.
[22]. M. Haupt, U. H. P. Fischer, Multi-colored WDM over POF system for triple-play, *Proceedings of SPIE*, Vol. 6992, 2008, 699213.
[23]. Y. Zhang, *et al.*, Study on coarse wavelength division multiplexing using polymer optical fiber transmission window, *Proceedings of the SPIE,* Vol. 5644, 2005, pp. 835-839.
[24]. U. H. P. Fischer, *et al.*, Demultiplexsystem für optische Datenübertragung mittels polymeroptischer Datenübertragung, in *Proceedings of the Nachwuchswissenschaftler Konferenz*, 2008.
[25]. H.-J. Thiele, M. Nebeling, Coarse Wavelength Division Multiplexing: Technologies and Applications, *CRC Press*, 2007.
[26]. , Product specification, 4, 8, and 16 Channel Extended Band CWDM Mux/Demux, *Lightel*, 2014.
[27]. A. K. Dutta, Dutta N K, M. Fujiwara, WDM Technologies: Passive Optical Components, *Acadamic Press*, 2003.
[28]. H. A. Macleod, Thin Film Optical Filters, 4th Ed., *CRC Press*, Taylor and Francis Group, 2010.
[29]. V. Herbert, Wavelength Filters in Fibre Optics, *Springer*, Berlin, Heidelberg, 2006.
[30]. L. V. Bartkiv, H. Poisel, A 3-channel POF-WDM system for transmission of VGA signals, in *Proceedings of the 12th International Conference on Plastic Optical Fibers*, 2003, pp. 264-270.
[31]. R. Kruglov, J. Vinogradov, O. Ziemann, S. Loquai, J. Müller, U. Strauß, C.-A. Bunge, Eye-safe data transmission of 1.25 Gbit/s over 100-m SI-POF using green laser diode, *IEEE Photonics Technol. Lett.*, Vol. 24, Issue 3, 2012, pp. 167-169.
[32]. S. Junger, W. Tschekalinskij, N. Weber, POF WDM transmission system for multimedia data, in *Proceedings of the 11th International Conference on Plastic Optical Fibers,* 2002, pp. 69-71.
[33]. W. Tschekalinskij, S. Junger, Optical multiplexer and demultiplexer for optical fibers with a large numerical aperture, European Patent, EP 1 532 477 B1, European Patent Office, 2010.
[34]. S. Junger, W. Tschekalinskij, N. Weber, POF WDM transmission system for multimedia data, in *Proceedings of the 11th International Conference on Plastic Optical Fibers,* 2002, pp. 69-71.
[35]. V. Appelt, J. Vinogradov, Simple FEXT compensation in LED based POF-WDM systems, in *Proceedings of the 11th International Conference on Plastic Optical Fibers,* 2002, pp. 127-129.
[36]. R. Kruglov, J. Vinogradov, O. Ziemann, S. Loquai, C.-A. Bunge, 10.7-Gb/s discrete multitone transmission over 50 m SI-POF based on WDM technology, *IEEE Photonics Technol. Lett.*, Vol. 24, Issue 18, 2012, pp. 1632-1634.
[37]. U. H. P. Fischer, M. Jončić, Wavelength division demultiplexer employing thin-film interference filters for the visible range, in *Proceedings of the 7th International Conference on Optics, Photonics and Lasers (OPAL'24)*, 2024, pp. 14-18.